JOURNAL OF MATERIALS SCIENCE 35 (2000) 3207–3211

Simulation of composite fatigue resulting from chemical attack of bridging fibers

D. N. COON, A. S. MOTKUR
Department of Mechanical Engineering, University of Wyoming, Laramie, WY 82072
E-mail: dcoon@uwyo.edu

A numerical simulation that predicted fatigue-like behavior resulting from chemical attack of bridging fibers in a cracked composite was developed. Chemical attack of bridging fibers led to mechanical failure of bridging fibers, and a corresponding reduction in the closure stress. As the closure stress decreased, the crack grew to form new bridging fibers. Crack growth rates were predicted to increase linearly with increased applied stress, and a fatigue exponent of 0.62 ± 0.06 was predicted. The predicted fatigue exponent was approximately an order of magnitude less than fatigue exponents reported for SiC/SiC composites in the literature. The low predicted fatigue exponent may indicate that mechanisms other than chemical attack of bridging fibers are operable in high-temperature experiments reported in the literature.

1. Introduction

High specific strength, stiffness, and toughness of ceramic matrix composites make them ideal candidates for high-temperature structural applications. The resistance of brittle materials to tensile failure is enhanced considerably by reinforcing with high strength fibers, such as SiC fibers. The micromechanisms that lead to improved fracture resistance include microcrack toughening, transformation toughening, and fiber bridging [1, 2]. Fibers bridging crack surfaces has been reported as a very effective mechanism in improving the resistance of brittle materials to failure [1].

Limited lifetimes under applied load and temperature have been experimentally observed for SiC fiber reinforced ceramic matrix composites [3–8], and several degradation mechanisms have been identified including fiber/environment reaction, creep, and wear of fiber surfaces during cyclic loading. Microstructural evidence of fiber damage in failed specimens consistent with chemical attack has been reported [9]. However, only a relatively small fraction of the fibers in any single sample showed evidence of substantial attack.

Chemical reactions of SiC fibers in oxidizing environments have been reported [9–14], and were generally related to attack of fiber coatings. Two common fiber coatings are carbon and BN. The presence of CO/CO_2 species in the environment has been shown to lead to chemical attack of carbon coated SiC fibers at temperatures as low as 400 °C [9, 13–14]. BN coatings that are not fully crystalline have been reported to be susceptible to oxidation at temperature $\geq$650 °C. The oxidation of fibers has been reported in ceramic matrix composites when applied tensile stress are high enough to result in matrix cracking [14]. The purpose of this communication is to report the numerical simulation of chemical attack of bridging fibers in a cracked composite, and determine if such reaction would result in fatigue-like behavior.

2. Numerical approach

The simulation described in this communication modeled quasi-static crack growth resulting from chemical attack of bridging fibers in a rectangular tow that was externally loaded. It was assumed that 492 fibers were uniformly positioned within a rectangular composite (12 Fibers by 41 fibers). A schematic representation of the composite containing a matrix crack and bridging fibers is shown in Fig. 1. Fibers to the left of the crack tip are bridging fibers.

Fig. 2 shows the flow chart of the computer simulation to model the effect of chemical attack of bridging fibers. The details of chemical reaction analysis have been previously reported [15]. The computer simulation was comprised of three main components: preprocessor, crack growth, and chemical reaction. The chemical and physical characteristics of individual fibers were determined and verified using Monte Carlo methods. The details of the development and verification of the Monte Carlo variables has been previously reported [15]. The Monte Carlo parameters used in this study are given in Table I. Crack growth was modeled using the principles of fracture mechanics. Bridging fibers carried loads that diminished the effect of external loads. The influence of the bridging fibers was determined from:

$$\sigma_{\text{bridge}} = \frac{F_{\text{bridge}}}{(12C)(4\bar{r})^2} \tag{1}$$

Where σ_{bridge} = effective bridging stress, F_{bridge} = sum of forces carried by bridging fibers, C = column location of crack tip, $\bar{r}$ = mean fiber radius.

TABLE I Monte Carlo variables used in the present study

Characteristic	Mean	Standard deviation	Weibull modulus	Characteristic strength	Ref.
Fiber radius	6.9 υm	1.3 υm			17, 18
Fiber modulus	145 GPa	30 GPa			19
Fiber strength			3.6	1.1 GPa	17, 18
Reaction rate	1% per timestep	$\pm$.1%			15
Force distribution exponent	2	$\pm$1			15
Fracture Toughness	4.0 MPa·m$^{1/2}$	0 MPa·m$^{1/2}$			1, 2

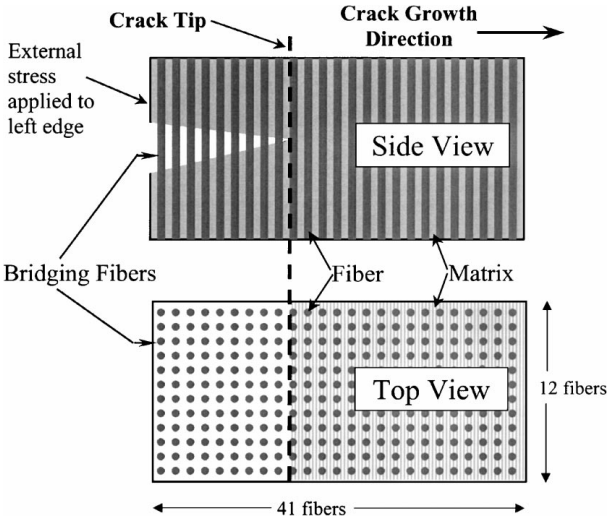

Figure 1 Schematic representation of composite system containing crack bridged by fibers.

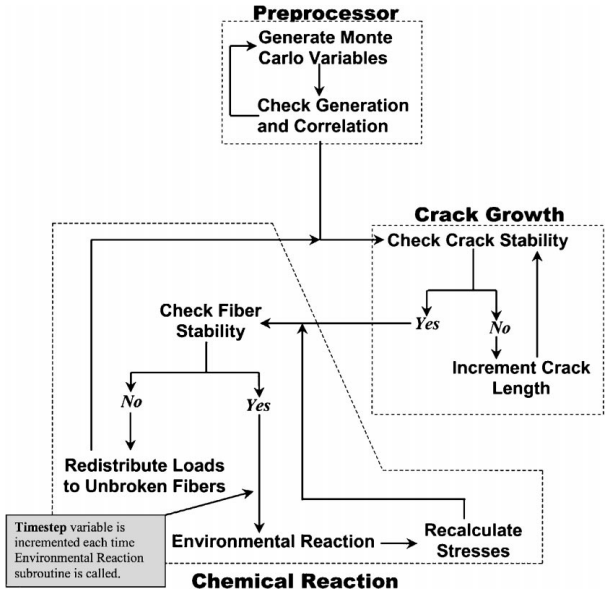

Figure 2 Flow chart of computer simulation of chemical attack of bridging fibers showing the relationship between the three components.

A planar crack front and a uniform fiber spacing of twice the mean fiber diameter was assumed in the development of Equation 1. The effective stress intensity factor for the cracked composite was calculated from:

$$K_{\mathrm{I}} = Y(\sigma_{\mathrm{applied}} - \sigma_{\mathrm{bridge}})\sqrt{4\pi \bar{r} C} \qquad (2)$$

Where K_{I} = effective stress intensity factor, $\sigma_{\mathrm{applied}}$ = external applied stress, Y = geometry constant ($\pi^{1/2}$ for an edge loaded surface crack).

The stability of the crack was determined by comparing the stress intensity factor to the fracture toughness using the following stability conditions:

$K_{\mathrm{I}} < K_{\mathrm{Ic}}$ ***Stable***—no crack extension expected

$K_{\mathrm{I}} \geq K_{\mathrm{Ic}}$ ***Unstable***—crack extension expected

If the crack was determined to be unstable, the crack length was increased by one column, and twelve new bridging fibers were created. Additional bridging fibers decreased the effective stress intensity even though the crack length increased slightly. This process was repeated until the crack was stable.

Once crack stability was attained, the bridging fibers were chemically attacked. This chemical attack resulted in a reduction in radii of bridging fibers. The mechanical stability of individual fibers was determined by comparing the fiber stress to the fiber strength [15]. As bridging fibers failed, the load was redistributed to remaining fibers based on position [15]. The combination of crack growth to maintain stability and chemical reaction of bridging fibers was repeated until all fibers failed. It should be noted that the matrix was assumed to be non-load bearing, and load from failed fibers was distributed only to fibers. This assumption simplified the computer simulation described in this study.

3. Results

The number of simulation results necessary to provide meaningful information is always a concern with Monte Carlo simulations. The rate of convergence of the simulation reported in this study was determined, and is shown in Table II. The simulation converged very rapidly, and a set of 5 simulation results provided information equivalent to a set of 100 simulation results.

TABLE II Test for convergence of simulation used an applied stress of 10% of the characteristic fiber strength

Number of simulation results	Mean lifetime	Standard deviation of lifetime
5	144.4	10.4
25	144.9	10.5
50	145.9	13.0
100	144.1	10.8

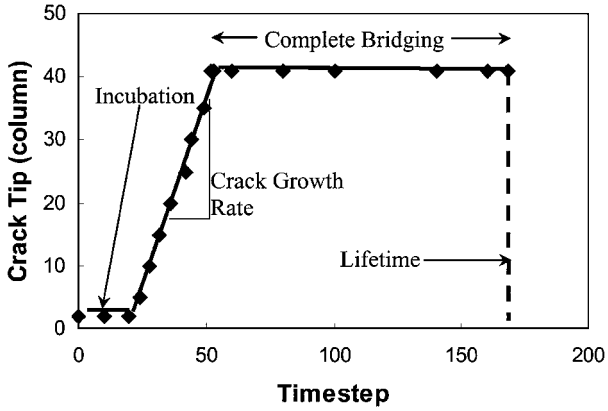

Figure 3 Typical results for an individual simulation of crack growth in a composite resulting from chemical attack of bridging fibers.

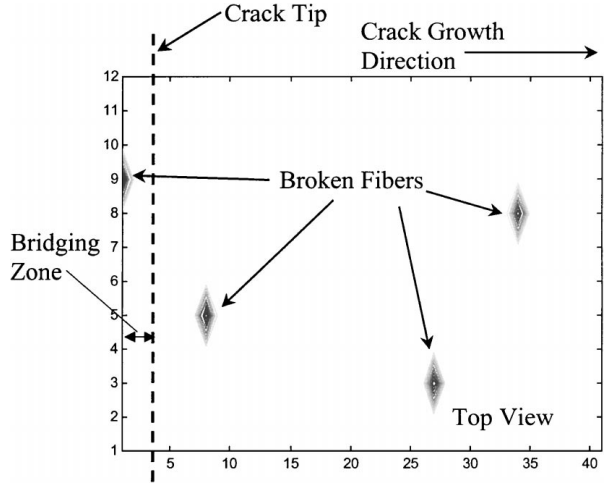

Figure 4 Mechanical state of fibers on initial mechanical loading with no chemical reaction.

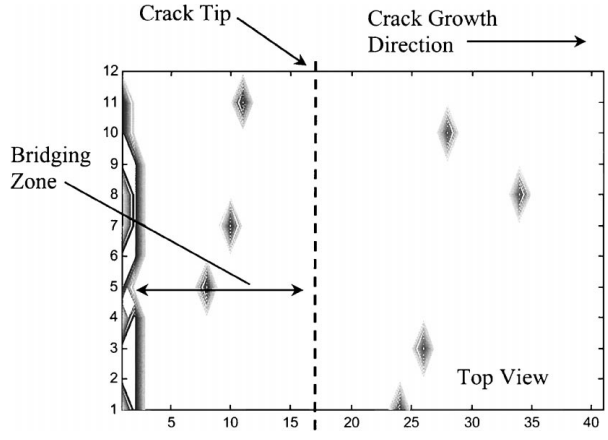

Figure 5 Mechanical state of fibers at an intermediate stage (after chemical attack of bridging fibers has resulted in crack growth).

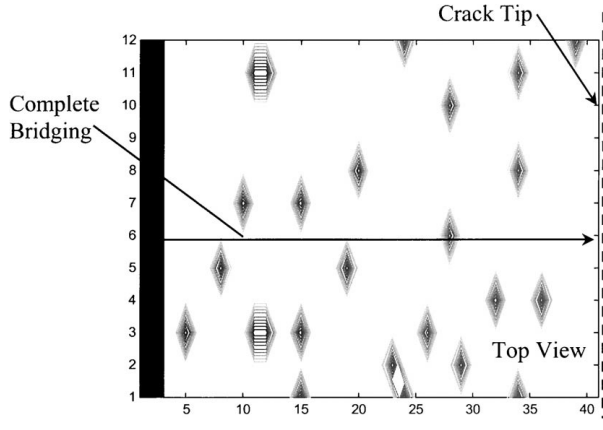

Figure 6 Mechanical state of fibers in the region of complete bridging.

Therefore, all data sets described in this communication were based on 5 simulation runs.

Typical results for an individual simulation are shown in Fig. 3 with crack position (column position of crack tip) plotted as a function of timestep (number of iterations through the environmental reaction subroutine). Several distinct regions are apparent in Fig. 3. At low numbers of timesteps, the crack position is constant. This region was labeled incubation, and resulted from an initial amount of chemical reaction necessary to cause the failure of sufficient bridging fibers. Only after sufficient bridging fibers had failed did the crack extend due to instability. The second region was the crack growth region, and was observed as in increase in crack position as a function of timestep. During this crack growth region, the crack extended as a resulted of continued chemical attack of bridging fibers. The third region occurred once the crack extended completely across the composite (crack position of 41). During this third stage, known as complete bridging, the two crack surfaces were held together by any fibers that remained. The simulation then continued chemical attack of all remaining fibers until all fibers had failed. The lifetime of the composite was determined as the point where all fibers failed. Typically, the incubation period lasted for 25–75 timesteps, and complete bridging occurred after approximately 10% of the fibers failed.

Fig. 4 shows the mechanical state of fibers on initial mechanical loading after crack stability has been attained at the beginning of the incubation stage (no chemical attack of bridging fibers). The triangular regions indicate broken fibers. The initial mechanical loading had the effect of breaking the weak fibers in the composite, and it was expected that 1–2 percent of fibers would fail on this initial loading [16]. The position of broken fibers was random throughout the composite, and this random fiber failure was expected from a Monte Carlo approach [15]. The crack tip (dashed vertical line) was set initially to 10% of the composite dimension, and this system was determined to be stable. All fibers to the left of the dashed were bridging fibers.

Fig. 5 shows the mechanical of fibers at an intermediate stage in the crack growth region, with the crack tip position approximately one-third of the way across the composite and approximately 5% of the fibers have failed. A larger fraction of the fibers in the original bridging zone near the left-hand edge have now broken. Additional fibers ahead of the crack tip have broken. It is interesting to note that fibers ahead of the crack are not exposed to the environmental reaction and have broken from purely mechanical response.

Fig. 6 shows the mechanical state of the fibers at the onset of the complete bridging stage, and the crack tip position was column 41. All fibers were now bridging

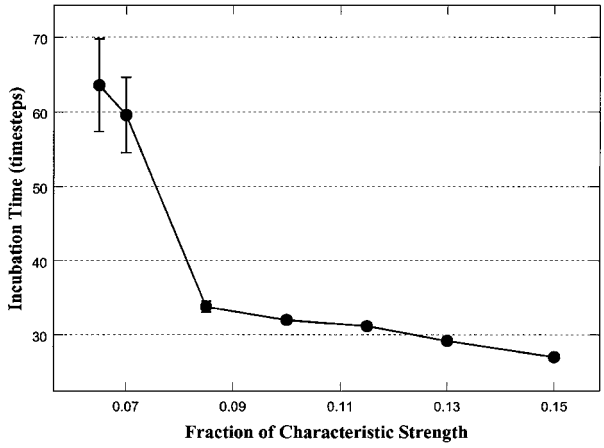

Figure 7 Effect of applied stress on the length of the incubation stage. The data points are the average of 5 simulation results and the error bars are standard errors of the mean.

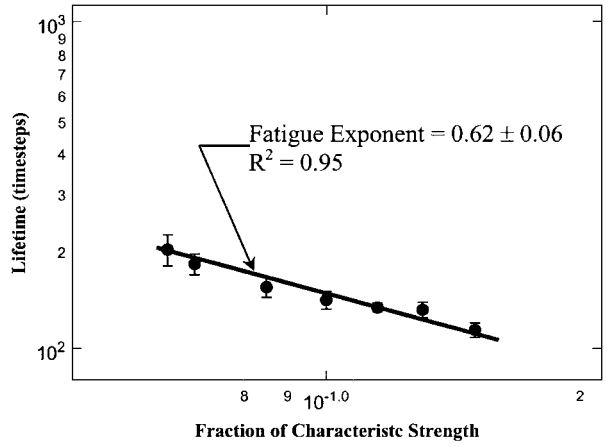

Figure 9 Fatigue plot of simulation results for chemical attack of bridging fibers. The data points are the averages of 5 simulation results and the error bars are standard errors of the mean.

fibers, and all fibers were exposed to the environmental reaction. Approximately 10% of the fibers have failed, but a region of complete failure now exists in the original bridging zone near the left edge. For the remainder of the lifetime, crack extension had completed, and the composite behavior was dominated by fiber reaction and corresponding failure [15].

The effect of applied stress ranging from 6.5% to 15% of the characteristic fiber strength on the length of the incubation stage is shown in Fig. 7. Long incubation periods and highly variable lengths were evident at the two lowest levels of applied stress. At higher levels of applied stress, the length of the incubation stage gradually decreased in a linear manner with increased applied stress. In addition, the length of the incubation stage was much more consistent at higher levels of applied stress.

Fig. 8 shows the effect of applied stress on the crack growth rate in the crack growth region. Relatively high crack growth rates were predicted for the two lowest stress values. At higher stress values, the crack growth rates increased in a gradual linearly manner with increased stress levels. Since the two lowest stress values resulted in a prolonged incubation stage, the relatively high crack growth rates for these stress levels is thought to result from significant chemical attack of bridging fibers prior to the onset of crack growth.

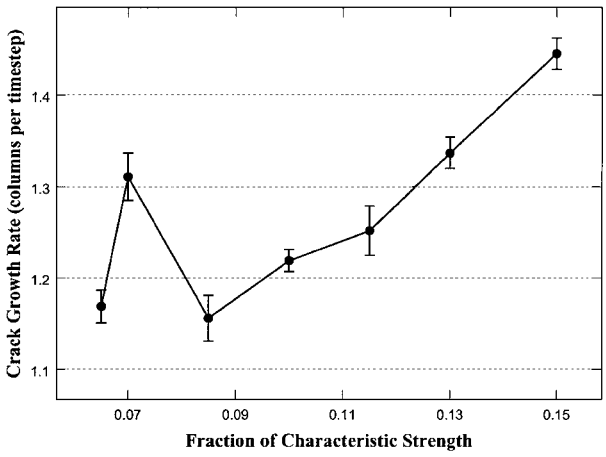

Figure 8 Effect of applied stress on the crack growth rate in the crack growth stage. The data points are the averages of 5 simulation results and the error bars are standard errors of the mean.

Fatigue behavior is typically demonstrated by the following characteristic equation:

$$t_{\text{life}} = A(\sigma_{\text{applied}})^n \tag{3}$$

Where t_{life} = lifetime, A = fatigue constant, σ_{applied} = applied stress, n = fatigue exponent.

The simulation results for applied stress levels ranging 6.5% to 15% of the characteristic strength are plotted in Fig. 9 according to the linear transformation of Equation 3. The Fatigue exponent was calculated to be 0.62 ± 0.06 with an R^2 value of 0.95. While simulation results indicate fatigue-type behavior was predicted for chemical attack of bridging fibers, the predicted fatigue exponent was approximately an order of magnitude lower than those observed experimentally observed for SiC/SiC composites [5, 6]. Three possible explanations for the difference in predicted and observed fatigue exponent exists. First, the simulation reported in this study assumed that the matrix phase did not carry mechanical load, i.e. all load was carried by fibers. In SiC/SiC composites, the matrix phase can indeed will carry some of the applied load. Second, a simple model of the effect of bridging fibers was used in the present study. A nonlinear effect based on the strain in individual fibers [1, 2] may be more appropriate. Third, additional mechanical response mechanisms, i.e. creep, may be operable in SiC/SiC composites.

4. Conclusions

A numerical simulation predicted that fatigue-like behavior would result from chemical attack of bridging fibers in a cracked composite. Monte Carlo techniques were use to develop fiber characteristics, and stochastic parameters were based on reported literature values. The rate of reaction with environmental species was chosen at a level to permit observation of fiber failure during the simulation. Chemical attack of bridging fibers led to mechanical failure of bridging fibers, and

a corresponding reduction in the bridging stress. As the bridging stress decreased, the crack grew to form new bridging fibers. Crack growth rates were predicted to increase linearly with increased applied stress. Crack growth was typically observed when approximately 5% of the fibers had failed, and crack growth continued until the crack extended throughout the composite. At this point, the crack surfaces were completely bridged, and the composite behavior was dominated by chemical reaction of all remaining fibers. Approximately 10% of the fibers had failed at the development of a completely bridged crack. A fatigue exponent of 0.62 ± 0.06 was predicted. This predicted fatigue exponent was approximately an order of magnitude less than fatigue exponents reported for SiC/SiC composites. The lower predicted fatigue exponent may indicate that other mechanisms are operable in high-temperature experiments reported in the literature.

References

1. D. B. MARSHALL and A. G. EVANS, in "Fracture Mechanics of Ceramics—Vol. 7," edited by R. C. Bradt, A. G. Evans, D. P. H. Hasselman and F. F. Lange (Plenum Press, 1986) p. 1.
2. A. G. EVANS and D. B. MARSHALL, in "High Temperature/High Performance Composites," edited by F. D. Lemkey, S. G. Fishman, A. G. Evans and J. R. Strife (Materials Research Society, 1988) p. 213.
3. L. P. ZAWADA, L. M. BUTKUS and G. A. HARTMAN, *Journal of the American Ceramic Society* **74**(11) (1991) 2851.
4. S. RAGHURAMAN, J. F. STUBBINS, M. K. FERBER and A. A. WERESZCZAK, *Journal of Nuclear Materials* **212/215** (1994) 840.
5. M. H. HEADINGER, P. GRAY and D. H. ROACH, Presented at the Composites and Advanced Structures Cocoa Beach Conference, Jan. 1995.
6. M. J. VERILLI, A. M. CALOMINO and D. N. BREWER, Presented at the Composites and Advanced Structures Cocoa Beach Conference, Jan. 1996.
7. H. T. LIN, P. F. BECHER, K. L. MORE, P. F. TROTORELLI and E. LARA-CURZIO, "Evaluation of Stress-Temperature-Lifetime Working Envelop for Enhanced Nicalon-SiC CFCC's." Oak Ridge Laboratory, 1996.
8. E. Y. SUN, S. T. LIN and J. J. BRENNAN, *Journal of the American Ceramic Society* **80**(3) (1996) 3065.
9. S. M. JOHNSON, R. D. BRITTAIN, R. LAMOREAUS and D. J. ROWECLIFFE, *ibid.* **71**(3) (1988) C132.
10. B. W. SHELDON, E. Y. SUN, S. R. NUTT and J. J. BRENNAN, *ibid.* **79**(2) (1996) 539.
11. R. T. BHATT, *ibid.* **75**(2) (1992) 405.
12. D. P. PLUCKNETT and M. H. LEWIS, *Journal of Materials Science Letters* **14** (1995) 1223.
13. L. FILIPUZZE, G. CAMUS and R. NASLAIN, *Journal of the American Ceramic Society* **77**(2) (1994) 449.
14. L. U. J. T. OGBUJI, *ibid.* **81**(11) (1998) 2777.
15. D. N. COON and A. M. CALOMINO, Accepted for Publication in the *Journal of Materials Science*, 1998.
16. D. N. COON, Under Review by the *ibid.* 1999.
17. A. J. ECKEL and R. C. BRADT, *Journal of the American Ceramic Society* **72**(3) (1989) 455.
18. G. SIMON and A. BUNSEL, *Journal of Materials Science* **19** (1984) 3649.
19. R. S. ZIMMERMAN and D. F. ADAMS, NASA Report No. 177525, April, 1989.

Received 11 August
and accepted 10 December 1999